

# PriorCVAE: scalable MCMC parameter inference with Bayesian deep generative modelling

**Elizaveta Semenova**

*Department of Computer Science  
University of Oxford*

*elizaveta.p.semenova@gmail.com*

**Max Cairney-Leeming**

*Department of Computer Science  
University of Oxford*

*max@cairneyleeming.co.uk*

**Seth Flaxman**

*Department of Computer Science  
University of Oxford*

*seth.flaxman@cs.ox.ac.uk*

## Abstract

In applied fields where the speed of inference and model flexibility are crucial, the use of Bayesian inference for models with a stochastic process as their prior, e.g. Gaussian processes (GPs) is ubiquitous. Recent literature has demonstrated that the computational bottleneck caused by GP priors or their finite realizations can be encoded using deep generative models such as variational autoencoders (VAEs), and the learned generators can then be used instead of the original priors during Markov chain Monte Carlo (MCMC) inference in a drop-in manner. While this approach enables fast and highly efficient inference, it loses information about the stochastic process hyperparameters, and, as a consequence, makes inference over hyperparameters impossible and the learned priors indistinct. We propose to resolve the aforementioned issue and disentangle the learned priors by conditioning the VAE on stochastic process hyperparameters. This way, the hyperparameters are encoded alongside GP realisations and can be explicitly estimated at the inference stage. We believe that the new method, termed PriorCVAE, will be a useful tool among approximate inference approaches and has the potential to have a large impact on spatial and spatiotemporal inference in crucial real-life applications. Code showcasing the PriorCVAE technique can be accessed via the following link: <https://github.com/elizavetasemenova/PriorCVAE>

## 1 Introduction

In applied fields where the speed of inference and model flexibility are crucial, the use of Bayesian inference for models with a stochastic process as their prior, e.g. Gaussian processes (GPs) is ubiquitous. GPs are used across a variety of fields, including environmental sciences (Dai et al., 2022), geosciences (Axen et al., 2022), agriculture (Belda et al., 2021), pharmaceutical industry (Obrezanova et al., 2007; Schroeter et al., 2007; Semenova et al., 2021; Shapovalova et al., 2022), remote sensing (You et al., 2017), robotics (Deisenroth et al., 2013), active learning (Krause & Guestrin, 2007) and others. They offer a powerful framework for defining distributions over functions (Williams & Rasmussen, 2006). A key benefit of GPs is their flexibility, which makes it possible to get consistent predictions at arbitrary locations from a trained model. However, the scope of real-world tasks that can be effectively tackled with GPs is limited due to the cost of inference. It scales as  $O(n^3)$  with respect to the number of observed datapoints,  $n$ , and characterisation of uncertainty via fully Bayesian inference is prohibitively computationally expensive.

Deep generative modelling is gaining traction across many fields, including geospatial applications (Wu & Biljecki, 2023). It has been recently demonstrated that generative models based on neural networks can

also learn distributions over tabular data (Hollmann et al., 2022) and functions (Dutordoir et al., 2022; Kerrigan et al., 2022). GP priors and a wider range of stochastic processes can be encoded, for example, using variational autoencoders (VAEs). Recently a group of two-stage methods has been proposed in the literature:  $\pi$ VAE (Mishra et al., 2022) encoding stochastic processes, and PriorVAE (Semenova et al., 2022) encoding realisations thereof. Both methods train a VAE on prior draws of a process at the first stage, and at the second stage, the trained decoder is used as a surrogate of the original GP for fully Bayesian inference using Markov chain Monte Carlo (MCMC). Neural networks are appealing since most of the computational effort is expended during the training process, while the task of inference becomes considerably faster and more efficient.

The PriorVAE method was originally introduced as a tool to solve the small area estimation (SAE) problem. SAE (Rao & Molina, 2015) of discrete spatial data, i.e. areal units, is important for policy and decision-making in fields that include epidemiology, environmental sciences, political polling and others. The SAE modelling usually takes place over a set of disjoint spatial areas  $A = \{A_i\}_{i=1}^n$  covering the domain of interest  $D = \bigcup_{i=1}^n A_i$ . The collection of such areas is referred to as *areal data*. Typically, it represents real-life administrative units. Some spatial units might not have samples readily available or the collected data might be noisy. Classical methods in spatial statistics use the multivariate normal (MVN) distribution to model areal data and rely on “borrowing strength” across neighbouring areal units. Despite the original intent to tackle SAE, PriorVAE is equally applicable to modelling of *geostatistical* data, which consists of observations at fixed in space locations, and *point pattern* data, which consists of locations of observed events. Both geostatistical and point pattern data are typically modelled on a computational spatial grid  $G = \{g_i\}_{i=1}^n$  using a GP with a MVN distribution of its realisations over  $G$ . Classical spatial statistics prescribes its own set of models to each of the three types of spatial data, and it is remarkable that PriorVAE offers a unified approach to treating them. Due to this shared setup enabled by PriorVAE, further in the text we will use the “GP” notation interchangeably with “MVN”. The essence of the PriorVAE method is that it substitutes realisations of the GP prior at the inference stage with the trained decoder leading to fast and highly efficient spatial inference, and already a fairly simple VAE architecture can make a measurable impact on approximating computationally cumbersome GPs. There is, however, one serious drawback of this approach: while  $\pi$ - and PriorVAE encode function values, both methods lack the ability to explicitly estimate hyperparameters. In some cases it is possible to retain explicit inference of the marginal variance, but this is not possible for the lengthscale even of the simplest kernels, or for the cases when kernels have more complex non-separable structure. In the present work we propose to overcome this issue with the conditional variational autoencoder (CVAE) architecture.

VAEs (Kingma & Welling, 2013) are a class of deep generative models which can generate new samples from a given data distribution. They do this by learning a compact, lower-dimensional representation of the data, i.e. the latent space, and then use this latent space to generate new samples. A VAE is trained by maximising the likelihood of the data under the learned model, while also imposing a regularization term that encourages the latent space to have a simple, well-behaved distribution. A CVAE Sohn et al. (2015) combines the capabilities of VAEs with the ability to condition the generated samples on external information, traditionally, the true observed label; it is a conditional directed graphical model whose input observations modulate the prior on the latent variables that generate the outputs. To train a CVAE, both the reconstruction and regularisation parts of the loss are conditioned on the additional information. Once the CVAE is trained, one can query samples corresponding to specific values of the condition.

In this work we propose to use CVAEs to learn priors, rather than observed data, and use hyperparameters of the priors for conditioning. This approach retains the advantages of PriorVAE at the inference stage, i.e. shorter computation times, higher effective sample size and training on unlimited amounts of noiseless data, while it also disentangles priors and allows an MCMC to explicitly estimate hyperparameters. We term the new method PriorCVAE and believe that it has the potential to make impact on the field of spatial and spatiotemporal inference by introducing a new class of approximate GP models. The new prior can be easily implemented and incorporated into custom probabilistic models of deliberate complexity in popular probabilistic programming languages such as Stan (Carpenter et al., 2017), NumPyro (Phan et al., 2019), PyMC3 (Bingham et al., 2019), Turing.jl (Ge et al., 2018) and others.

Our contributions can be summarised as follows:

- We extend the PriorVAE method to “disentangle” the learned priors by introducing the conditional variational autoencoder architecture, allowing us to explicitly encode hyperparameters and estimate them at the inference stage,
- We demonstrate for the first time that the method is applicable to GPs with non-stationary kernels,
- We demonstrate that PriorCVAE is able to extrapolate with respect to hyperparameters, i.e. we can draw priors for values of hyperparameters which the CVAE has not been trained on,
- We introduce an additional training hyperparameter allowing to improve calibration of the decoder by utilising a more rigorous statistical approach to VAE reconstruction loss,
- We perform empirical comparison of four different approximate methods: Laplace approximation, ADVI, PriorVAE and PriorCVAE using the same implementation software,
- We show that properties of functions obtained via non-linear transformations of function values can be learned alongside function evaluations.

The rest of this paper is organised as follows: in Section 2 we present related work and summarise the methodology of the previously existing two-stage approaches, and in Section 3 we present the novel PriorCVAE method. In Section 4 we present a range of experiments using the new method, demonstrating its capabilities on simulated and real-life data. We conclude with a discussion of these results in Section 5 and provide a broader outlook on the potential impact of this work and future research directions.

## 2 Related Work

In this section we provide motivation for using MCMC as a reliable tool for Bayesian inference, introduce deep generative models, summarise VAE and CVAE architectures, and describe the PriorVAE and  $\pi$ VAE methods.

### 2.1 Markov Chain Monte Carlo

In the Bayesian inference setting, we are interested in learning the probability distribution of a set of unknown parameters or latent variables  $z$  given observed data  $y$  defined by their joint distribution  $p(y, z) = p(y|z)p(z)$ , where  $p(y|z)$  is the *likelihood* of the observed data and  $p(z)$  is the *prior* of the latent variable  $z$ . The *posterior* of the latent variable is then formed as  $p(z|y) \propto p(y|z)p(z)$ . MCMC is a general sampling technique for sampling from a, possibly, unnormalised target density  $\pi(z)$ , i.e. the posterior (Robert et al., 1999; Gelman et al., 1995). MCMC simulates an ergodic Markov chain  $\{z^{(i)}\}_{i \in \mathbb{N}}$  that admits  $\pi(z)$  as its unique limiting distribution. In practice, the simulation is performed for a finite number of iterations  $N$ , where  $N$  is sufficiently large for MCMC to converge. MCMC convergence and efficiency can be assessed via diagnostic tools, such as the R-hat statistic and effective sample size (ESS) metrics, correspondingly (Vehtari et al., 2021). The main advantage of MCMCs is that they provide guarantees of producing asymptotically *exact* samples from the target density. In applications where modelling informs decision making this property makes MCMC preferable to non-exact methods. While MCMC has proven to be very successful as compared to simpler inference algorithms due to its flexibility, it scales poorly for problems involving correlation structures, such as GPs and large spatial settings. Additional issues, inherent to MCMC itself, are auto-correlations of samples making sampling less efficient.

### 2.2 Variational inference

The goal of variational inference (VI) is to approximate a conditional density of latent variables given observed variables  $p(z|y)$  (Wainwright & Jordan, 2008; Blei et al., 2017; Wainwright et al., 2008) with a distribution  $q(z)$ . The approximating distribution  $q(z)$  is chosen from a variation family of simpler distributions  $\mathcal{Q}$  than the target by minimising the KL-divergence  $\min_{q(z) \in \mathcal{Q}} KL[q(z)||p(z|y)]$ . This problem statement effectively turns the inference problem into an optimisation problem allowing use of a range of modern optimisation

techniques. The aforementioned KL divergence is not tractable, since  $p(z|y)$  is not known, so instead we maximise the evidence lower bound (ELBO) with respect to  $q$ , since  $\log p(y) \geq \text{ELBO}$ , where  $\text{ELBO}(y) = \mathbb{E}[\log p(z, y)] - \mathbb{E}[\log q(z)]$ . VI does not enjoy such guarantees as MCMC and it can only find a density close to the target from the variational family. Variational family is usually chosen out of convenience and might be biasing estimates, but it tends to be faster than MCMC.

## 2.3 Deep generative modelling

A common shared principle behind generative neural networks (Bond-Taylor et al., 2021; Tomczak, 2022) is to start with an input constituted by samples from a simple probability distribution, such as i.i.d. Gaussian Normal  $z \sim \mathcal{N}(0, I)$ , and apply a generative model in the form of a neural network with trainable parameters, which transforms the simple noise distribution into samples from the probability distribution of interest. Such neural networks are trained on a set of representative samples from the distribution of interest. Hence, the training process needs to indirectly make inference about what this probability distribution is and how well the distribution produced by the generator matches the target distribution.

## 2.4 VAE

VAE (Kingma & Welling, 2013; Rezende et al., 2014) is a deep generative model allowing dimensionality reduction. Its architecture resembles deterministic autoencoders and consists of two feed-forward neural networks - an encoder  $E_\gamma(\cdot)$  and a decoder  $D_\psi(\cdot)$  (see Figure 11). The encoder  $E_\gamma(\cdot)$ , parameterised by  $\gamma$ , maps an input  $y \in \mathcal{Y} \subset \mathbb{R}^n$  into the latent space  $\mathcal{Z} \subset \mathbb{R}^d$ , where  $d$  is typically lower than  $n$ . The decoder network  $D_\psi(\cdot)$ , parameterised by  $\psi$ , aims to reconstruct the original data  $y$  from a sample from the latent space  $z \in \mathcal{Z}$  by generating  $\hat{y} = D_\psi(z)$ ,  $\hat{y} \in \mathcal{Y}$ . Therefore, this architecture imposes an ‘information bottleneck’ in the network which enforces a compressed representation  $z$  of the original input  $y$ . In contrast to a regular autoencoder, however, a VAE maps  $y$  not into a unique latent space vector, but instead to a probability distribution over it. To train a VAE, a variational approximation is used to estimate the posterior distribution  $p(z|y) \propto p(y|z) \times p(z)$ :  $p(z|y) \approx q(z|y)$ . Often the Gaussian probability model

$$q(z|y) = \mathcal{N}(\mu_z, \sigma_z^2 I_d)$$

is chosen as the model of the latent space, and its moments, or their bijective transformations, are learned by the encoder network:

$$\begin{aligned} (\mu_z, \log \sigma_z^2) &= E_\gamma(y), \\ z &\sim \mathcal{N}(\mu_z, \sigma_z^2 I_d). \end{aligned}$$

The prior distribution over  $z$ ,  $p(z)$ , is also chosen to have a simple Gaussian form, e.g.  $\mathcal{N}(0, I_d)$ . Following Kingma & Welling (2013), the optimal parameters for the encoder and decoder are found by maximising the evidence lower bound:

$$\mathcal{L}_{\text{VAE}} = \mathbb{E}_{q(z|y)} [\log p(y|z)] - \text{KL} [q(z|y) || p(z)].$$

The first term in the loss is the log-likelihood, which quantifies the quality of the reconstruction, i.e. how well the input  $y$  matches the output  $\hat{y}$ . The second term is the Kullback-Leibler divergence ensuring that  $z$  is as similar as possible to the prior, a  $d$ -dimensional standard Normal. This second part of the loss regularises the distribution of the latent space.

## 2.5 CVAE

Sohn et al. (2015) is an extension of the VAE where the entire generative process is conditioned on an additional input  $c$ , typically, a class label. Such conditioning allows us to control the class which we want the samples to be generated from (Figure 11). Therefore, CVAE can disentangle the produced reconstructions by introducing external knowledge, so that different categories are encoded separately, and thus the accurate latent variables can be sampled during random sampling. This alteration to VAEs allows us to tackle problems where the input-to-output mapping is one-to-many, without needing to explicitly specify the structure of the output. The optimised objective becomes

$$\mathcal{L}_{\text{CVAE}} = \mathbb{E}_{q(z|y,c)} [\log p(y|z, c)] - \text{KL} [q(z|y, c) || p(z|c)].$$

## 2.6 $\pi$ VAE and PriorVAE: encoding priors with VAEs

$\pi$ VAE (Mishra et al., 2022) and PriorVAE (Semenova et al., 2022) are two related VAE-based methods that are able to encode continuous stochastic processes and their finite realisations, respectively. They use the trained decoder as an approximation of computationally complex structures for Bayesian inference with MCMC. In this way, the rigour of MCMC is preserved, enabling inference of complex and expressive models, while the scalability of such models is ensured by the simple structure of the VAE’s latent space. The main conceptual difference between  $\pi$ VAE and PriorVAE is in the types of priors which they encode and the mechanics of such encoding.  $\pi$ VAE learns low dimensional embeddings of function classes by combining a trainable feature mapping with generative model using a VAE. The method is inspired by the Karhunen-Loève Expansion stating that any stochastic process  $f(s)$  can be represented as an infinite sum  $f(s) = \sum_{j=1}^{\infty} \beta_j \phi_j(s)$ , where  $\{\phi_j(\cdot)\}_{j=1}^{\infty}$  is a set of orthonormal basis functions and  $\{\beta_j\}_{j=1}^{\infty}$  are pairwise uncorrelated random variables. To train  $\pi$ VAE, the basis functions are learned via feed-forward neural network architecture over the input space, and random coefficients  $\beta_j$  are encoded using a VAE. The PriorVAE method was proposed as a scalable solution to the small area estimation (SAE) problem in spatial statistics. It encodes finite realisations of a Gaussian process and multivariate normal distributions widely used in spatial statistics. Such distributions are defined by the precision matrices based on the adjacency structure of the modelled areas and include conditional auto-regressive (CAR), intrinsic conditional auto-regressive (ICAR) and Besag-York-Mollié (BYM) models (Besag, 1974; Besag et al., 1991; Riebler et al., 2016). A characteristic property of PriorVAE is that it needs to be trained on a predefined spatial structure. On one hand, this is a disadvantage compared to  $\pi$ VAE since PriorVAE is unable to make predictions on off-grid locations. On the other hand, in the settings when the spatial structure is known in advance, PriorVAE is preferred due to its simpler computational setup, as only the prior-encoding VAE needs to be trained, without the need for learning of the feature map. The workflow of the PriorVAE method is as follows:

1. Fix the spatial structure of interest  $\{x_1, \dots, x_n\}$  - a set of administrative units, or an artificial computational grid.
2. Draw evaluations of a GP prior  $f \sim \mathcal{GP}(\cdot)$  over the spatial structure and use the vector of realisations  $f_{\text{GP}} = (f(x_1), \dots, f(x_n))^T$  as data for a VAE to encode.
3. Perform Bayesian inference of the overarching model using MCMC, where  $f_{\text{GP}}$  is approximated using the trained decoder  $D_{\psi}(\cdot)$ :

$$f_{\text{GP}} \approx \hat{f}_{\text{GP}} = f_{\text{PriorVAE}} = D_{\psi}(z_d), \quad z_d \sim \mathcal{N}(0, I_d).$$

## 3 Our contribution: inferring parameters via encoded priors

### 3.1 PriorCVAE: enabling parameter inference

PriorVAE is able to encode priors but suffers from a major drawback: it does not explicitly encode hyperparameters, which makes estimation of the hyperparameters impossible at the Bayesian inference stage. This feature is the main gap between these prior encoding methods and state-of-the-art approaches. It arises because the encoding network  $E_{\gamma}(f_{\text{GP}})$  encodes samples  $f_{\text{GP}}$ , but it cannot distinguish between samples generated given different values of hyperparameters. Similarly, the decoder  $D_{\psi}(z)$  only models  $f_{\text{GP}}$  directly using the variables  $z$ , and no additional condition. Hence, such decoders will produce priors corresponding to a wide range of hyperparameters, without any information about these hyperparameter values.

In some simple cases this issue can be bypassed. Consider a GP  $f \sim \mathcal{GP}(0, k)$  with a functional kernel  $k(\cdot, \cdot)$  where marginal variance is separable from other model hyperparameters  $\theta$ :

$$k(s_i, s_j) = \sigma^2 R_{\theta}(s_i, s_j),$$

where  $R_{\theta}$  is, for example, the radial basis function kernel (RBF) (Broomhead & Lowe, 1988),  $R_{\theta}(s_i, s_j) = \exp\left(-\frac{\|s_i - s_j\|^2}{2l^2}\right)$ , which has one parameter in  $\theta$ , the lengthscale  $l$ . Due to this separability, while training

a VAE, it is sufficient to encode "standardised" draws, i.e.  $\sigma = 1$ , so the priors to be encoded are drawn as  $f_{\text{std}} \sim \mathcal{GP}(0, k_{\text{std}})$ , where  $k_{\text{std}}$  is simply

$$k_{\text{std}}(s_i, s_j) = R_\theta(s_i, s_j).$$

At the inference stage the marginal variance  $\sigma^2$  can be estimated explicitly thanks to the relationship  $f = \sigma f_{\text{std}}$ . This trick is not possible in general and even in the RBF kernel example, information about the lengthscale  $l$  is completely lost during the VAE training. The issue is amplified further when working with even more complex cases, such as non-stationary kernels.

We propose a solution to this problem: a new method called PriorCVAE, which pairs the PriorVAE workflow with a CVAE architecture, replacing the VAE previously used. The encoder and decoder can now condition on the hyperparameters of the GPs, i.e.  $c = \theta$ , allowing us to generate approximate evaluations of the prior for specific hyperparameters, and also to perform inference on hyperparameters later on. The hyperparameters may be categorical or real-valued, allowing freedom of GP kernel choice.

One phenomenon noticed in the original PriorVAE model was imprecise learning of the second moments quantified as 90% Bayesian credible intervals (BCIs). This is a known behaviour for vanilla VAEs as they tend to produce blurred data. We remedy this artefact by introducing an additional tuning parameter. Rather than using traditional mean squared error (MSE) as the reconstruction loss, we utilise, instead, the original probabilistic formulation in the form of log-likelihood assuming that the reconstructed sample  $f_{\text{PriorCVAE}}$  is Normally distributed with the centre at  $f_{\text{GP}}$  and standard deviation  $\sigma_{\text{vae}}$ :

$$f_{\text{PriorCVAE}} \sim \mathcal{N}(f_{\text{GP}}, \sigma_{\text{vae}}^2).$$

Here  $\sigma_{\text{vae}}$  is a hyperparameter in the neural network training process which affects the amount of uncertainty learned by PriorCVAE and leads to better uncertainty calibration. The log-likelihood can be written as  $-\frac{1}{2\sigma_{\text{vae}}^2} \text{MSE}(f_{\text{GP}}, f_{\text{PriorCVAE}}) + c$ , and the full objective takes the form

$$\mathcal{L}_{\text{PriorCVAE}} = \frac{1}{2\sigma_{\text{vae}}^2} \text{MSE}(f_{\text{GP}}|\theta, f_{\text{PriorCVAE}}|\theta) - \text{KL} [\mathcal{N}(\mu_z, \sigma_z^2 I_d | \theta) || \mathcal{N}(0, I_d)] . \quad (1)$$

In this formulation, the inverse variance of the error term varies the weighting of reconstruction compared to the KL-term. This approach is closely related to  $\beta$ -VAE (Higgins et al., 2017) trained using the objective

$$\mathcal{L}_{\beta\text{-VAE}} = \frac{1}{2} \text{MSE}(y, \hat{y}) + \beta \text{KL} [q(z|y) || p(z)]$$

with the difference that in our formulation the weighting parameter is interpretable as it is linked to the amplitude of generated samples. The workflow of the PriorCVAE method is presented in Algorithm 1.

### 3.2 Why does it work?

The last step of the PriorCVAE workflow shown in in Algorithm 1 highlights the source of computational efficiency of the method. GP evaluations can be computed as

$$f_{\text{GP}}|\theta = L_\theta z_n, \quad z_n \sim \mathcal{N}(0, I_n),$$

where  $L_\theta$  is the Cholesky decomposition of covariance matrix  $K_\theta = L_\theta L_\theta^T$ . That is,  $z_n$  is linearly transformed to obtain  $f_{\text{GP}}|\theta$ , but the matrix  $L_\theta$  contains unknown parameters  $\theta$  which need to be inferred, and that causes  $O(n^3)$  complexity. PriorCVAE, instead, performs a non-linear transformation  $D_\psi(\cdot)$

$$f_{\text{PriorCVAE}}|\theta = D_\psi(z_d, \theta) \quad z_d \sim \mathcal{N}(0, I_d),$$

but of a smaller vector  $z_d$ ,  $d < n$ , and, most importantly, with fixed parameters  $\psi$ , which were learnt in the CVAE training step.

---

**Algorithm 1** PriorCVAE workflow

---

1. Fix the spatial structure of interest  $\{x_1, \dots, x_n\}$  - a set of administrative units  $A = \{A_1, \dots, A_n\}$ , or an artificial computational grid  $G = \{g_1, \dots, g_n\}$ .
2. Draw evaluations of prior  $f$  over the spatial structure governed by hyperparameters  $\theta$ :  $f \sim \mathcal{GP}_\theta(\cdot)$  over  $G$ , or  $f \sim \mathcal{MVN}_\theta(\cdot)$  over  $A$ .
3. Use the vector of realisations  $f_{\text{GP}} = (f(x_1), \dots, f(x_n))^T$  as data for a CVAE to encode, conditional on hyperparameters value  $c = \theta$ . Train PriorCVAE using the loss from Equation 1.
4. Perform fully Bayesian inference with MCMC of the overarching model, including latent variables and hyperparameters  $\theta$ , by approximating  $f_{\text{GP}}|\theta$  with  $f_{\text{PriorVAE}}|\theta$  in a drop-in manner using the trained decoder  $D_\psi(\cdot)$ :

$$f_{\text{GP}}|\theta \approx \hat{f}_{\text{GP}}|\theta = f_{\text{PriorVAE}}|\theta = D_\psi(z_d, \theta), \quad z_d \sim \mathcal{N}(0, I_d).$$

---

## 4 Experiments

### 4.1 Encoding lengthscale of a GP as a binary condition

**Priors to encode.** In the first example we work with a GP evaluated over a regular one-dimensional grid, consisting of  $n = 100$  points over the  $(0, 1)$  interval. Training samples from the prior are drawn as evaluations of a GP with zero mean and standardised ( $\sigma^2 = 1$ ) RBF kernel  $k_l^{\text{RBF}}(h) = \exp(-\frac{h^2}{l^2})^1$ , since, as we have shown above, marginal variance can be inferred separately and does not impact scalability. To allow for hyperparameter learning, we impose hierarchical structure on the model by using a hyperprior on the lengthscale  $l$ . The hyperprior chosen in this experiment is a discrete distribution with equal point masses at  $l_1 = 0.1$  and  $l_2 = 0.4$ . Hence, all generated draws will correspond to either of these two lengthscales. The lengthscale  $l$  can be parametrized via the *binary condition*  $c$  represented by a Bernoulli random variable. Therefore, the full hierarchical generative model takes the form

$$\begin{cases} c & \sim \text{Bernoulli}(0.5), \\ l|c & = (1 - c)l_1 + cl_2, \\ f|l & \sim \mathcal{GP}(0, k_l^{\text{RBF}}(\cdot, \cdot)) \end{cases} \quad (2)$$

and CVAE is trained on the samples of  $f$ , conditioned on  $l$ .

**Neural network training details.** We create training and test datasets, each of 100000 randomly sampled GP prior evaluations according to Equations 2. We follow the architecture used in Semenova et al. (2022), i.e. a multilayer perceptron (MLP). However, our experiments showed that even one hidden layer is enough to achieve performance similar to the one with two and more hidden layers under this architecture. Both the encoder and the decoder are MLPs and contain  $n_{\text{input}} = 100$  input (output for the decoder) nodes,  $n_h = 70$  hidden nodes, and the dimension of the latent space is  $n_z = 50$ . The model was trained for  $n_{\text{epochs}} = 250$  epochs, with  $n_{\text{batch}} = 1000$  batch size, and  $1e^{-3}$  learning rate using the Adam optimiser (Kingma & Ba, 2014). Value of the  $\sigma_{\text{vae}}^2$  hyperparameter was set to 0.9. Training of the neural network took 9 minutes.

**Learned priors.** The main characteristics of the input and learned priors are presented in Figure 1. We are now able to draw priors intentionally from one of the two classes, according to the condition supplied to the decoder. The figure empirically shows that the typical shape of priors, overall mean and uncertainty have been learned well. The empirical covariance matrices of the original GP and PriorCVAE priors also show similar patterns (Figure 12).

---

<sup>1</sup>Canonically, the RBF kernel is defined as  $\exp(-\frac{h^2}{2l^2})$ . We use a slightly different parametrisation of the lengthscale for simplicity.

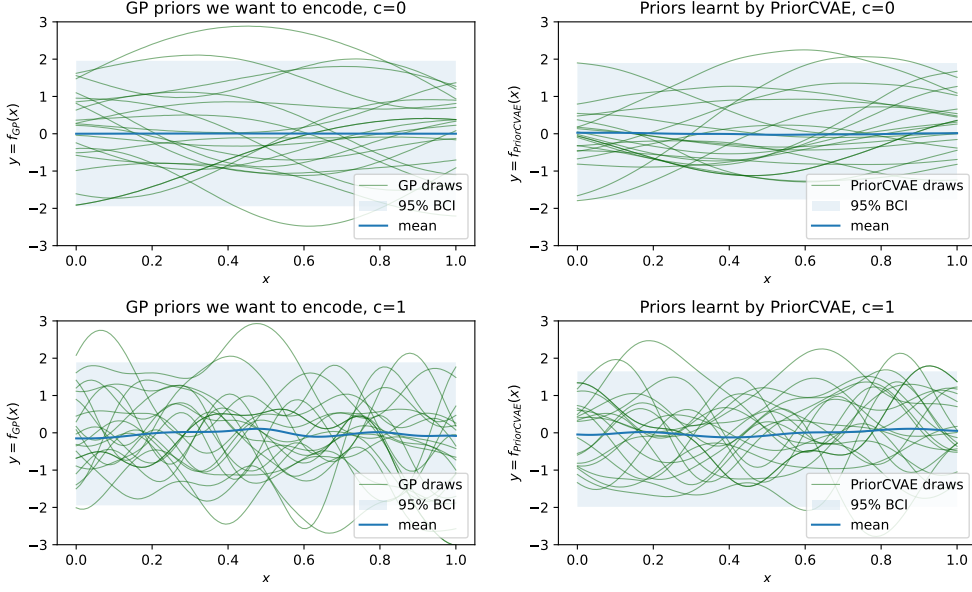


Figure 1: Visual diagnostics of the priors learned by PriorCVAE and the original GP priors corresponding to the standardised RBF kernel. Left column: samples, mean and 95% BCI from the original Gaussian process evaluations  $f_{GP}$ , right column: samples, mean and 95% BCI drawn from  $f_{\text{PriorCVAE}}$  trained on  $f_{GP}$  draws. Top row: condition  $c = 0$ , bottom row: condition  $c = 1$ .

**MCMC Inference.** To perform inference, we generate one GP realisation according to the true value of the condition  $c = 1$  and use it as the ground truth  $f_{\text{true}}$ . Seven observed data points are sampled by adding i.i.d. noise to the ground truth according to the half-Normal prior  $s \sim \mathcal{N}^+(0.1)$ :  $f_{\text{obs}} \sim \mathcal{N}(f_{\text{true}}, s)$ . Using this observed data we aim to reconstruct the underlying true curve according to three different scenarios: (a) assuming that the condition is known but false, (b) assuming a known and true condition, and (c) inferring the condition alongside reconstruction of the true trajectory. For all scenarios, we ran 4 MCMC chains with  $n_{\text{warmup}} = 1000$  steps, and  $n_{\text{samples}} = 100000$  post-warmup steps. Results of scenarios (a) and (b) are presented in Figure 2; inference in both cases was performed using a NUTS sampler (Hoffman & Gelman, 2014) and took 8 seconds and 30 seconds, correspondingly. Scenario (c) needs a separate treatment as direct inference of discrete parameters, such as  $c \in \{0, 1\}$ , is impossible with NUTS. Instead, we use two alternative approaches. The first approach is to approximate the discrete distribution of the condition with a Beta-prior  $c \sim \text{Beta}(10^{-4}, 10^{-4})$  which is concentrated around values 0 and 1 and assigns low probability away from 0 and 1. This model is inferred using NUTS (see Figure 3, left) and took 24 seconds to run. The second approach is to assign  $c$  its original discrete prior  $c \sim \text{Bernoulli}(0.5)$  and use the MixedHMC sampler (Zhou, 2020) (see Figure 3, right); it took 9 minutes to run. The results are very close to those when the true condition value is known (Figure 3, left), and the posterior samples of  $c$  obtained using the two approaches are shown on the bottom of Figure 3.

## 4.2 Continuous condition: PriorVAE vs PriorCVAE

**Priors to encode.** This experiment builds on the example of a binary condition presented in Section 4.1 and encodes the lengthscale of a GP as a continuous condition  $c = l$ . The prior generating setup is similar to the one above: we work on a regular one-dimensional grid of  $n = 80$  points over the  $(0, 1)$  interval and draw samples according to the standardised RBF kernel. However, this time the lengthscale is randomly drawn from the uniform prior distribution over the interval  $(0.01, 0.99)$ :

$$\begin{cases} l & \sim \mathcal{U}(0.01, 0.99), \\ f|l & \sim \mathcal{GP}(0, k_l^{\text{RBF}}(\cdot, \cdot)). \end{cases} \quad (3)$$



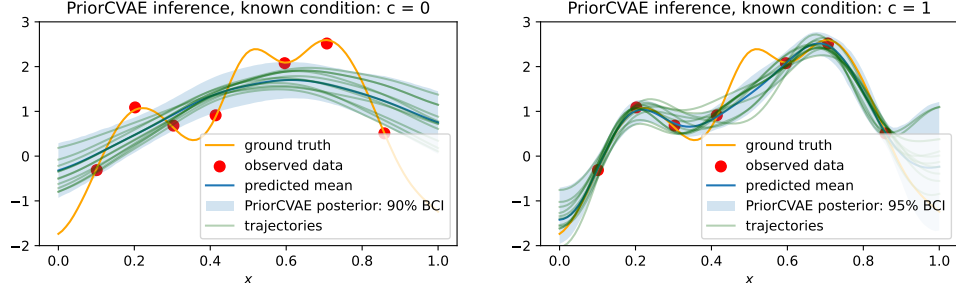


Figure 2: Inference performed using NUTS and PriorCVAE, assuming the binary condition  $c$  is known. Left:  $c = 0$  (misspecified model), right:  $c = 1$  (correctly specified model).

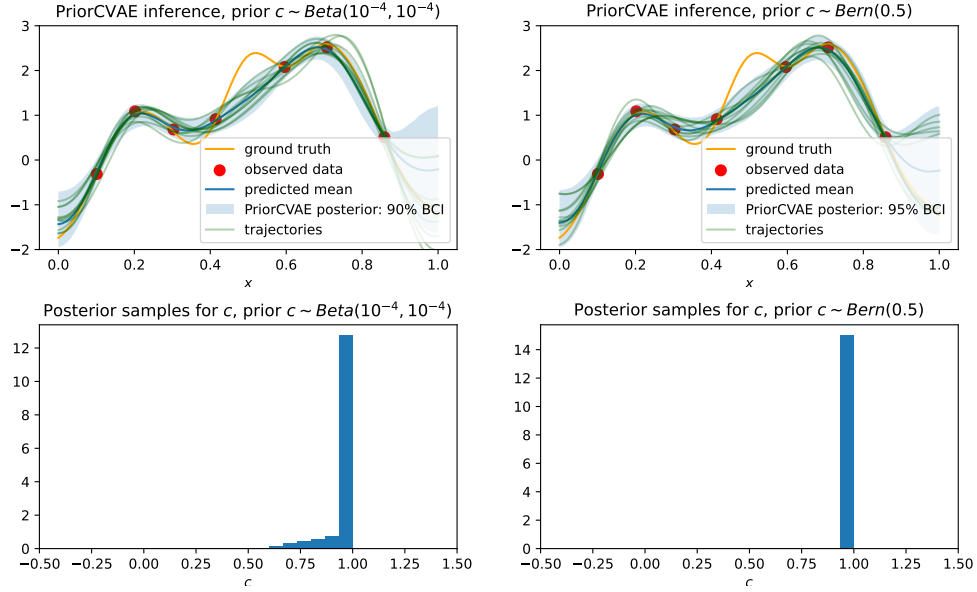


Figure 3: Left: inference performed using NUTS and PriorCVAE with a binary condition, approximating the true Bernoulli prior with a continuous Beta prior. Right: inference performed using MixedHMC and PriorCVAE with a binary condition, inferred as a discrete variable with a Bernoulli prior.

This is a very conservative prior, as in practice more informative priors are commonly used, such as an Inverse-Gamma.

**Training PriorVAE and PriorCVAE.** We create training and test datasets, each of 100000 randomly sampled GP prior evaluations according to Equations 3. In order to perform one-to-one comparison of PriorVAE and PriorCVAE we opt to keep the train and test sets fixed (as opposed to generating data on the fly during the training process). The architecture of the two models is also identical: both the endcoder and the decoder are MLPs with one hidden layer and  $n_{\text{input}} = 80$  input (output for the decoder) nodes,  $n_h = 60$  hidden nodes, and the dimension of the latent space is  $n_z = 40$ . Both models were trained for  $n_{\text{epochs}} = 400$  epochs, with  $n_{\text{batch}} = 1000$  batch size, and  $1e^{-3}$  learning rate using the Adam optimiser. Training time of both neural networks was 23 minutes. Comparing the training and test losses of the two models already provides insights into which of the two is able to describe the data better (Figure 13): both the test and training losses of PriorCVAE are lower than those for PriorVAE throughout the training process.

**Learned priors.** Figure 4 compares three sets of priors: those obtained by GP ( $f_{\text{GP}}$ , top row), PriorVAE ( $f_{\text{PriorVAE}}$ , middle row) and PriorCVAE ( $f_{\text{PriorCVAE}}$ , bottom row). Priors in the left column are conditioned on a short lengthscale  $l = 0.1$ , and on the right on a long lengthscale  $l = 0.9$ .  $f_{\text{PriorCVAE}}$  priors closely resemble original  $f_{\text{GP}}$  priors, while  $f_{\text{PriorVAE}}$  priors are inflexible. This phenomenon certainly has an effect at the inference stage: not only is PriorCVAE able to explicitly encode the lengthscale parameter, it also allows for the parameter to be inferred, as opposed to the entangled  $f_{\text{PriorVAE}}$  priors. The empirical covariance matrices  $K_{\text{PriorVAE}}$ ,  $K_{\text{PriorCVAE}}$  corresponding to the same set of priors are presented in Figure 5; we quantify the distance between the empirical covariance matrices obtained from PriorVAE and PriorCVAE priors  $K_{\text{PriorVAE}}$ ,  $K_{\text{PriorCVAE}}$  to the one obtained from GP draws  $K_{\text{GP}}$  by calculating the Frobenius norms  $F_{\text{PriorVAE}} = \|K_{\text{GP}} - K_{\text{PriorVAE}}\|_F$ ,  $F_{\text{PriorCVAE}} = \|K_{\text{GP}} - K_{\text{PriorCVAE}}\|_F$ , which are presented in Table 1.

Table 1: Quantification of the quality of the learned priors: Frobenius norms measure the distance between empirical covariance matrices obtained from the original GP prior, and learned PriorVAE and PriorCVAE priors  $F_{\text{PriorVAE}} = \|K_{\text{GP}} - K_{\text{PriorVAE}}\|_F$ ,  $F_{\text{PriorCVAE}} = \|K_{\text{GP}} - K_{\text{PriorCVAE}}\|_F$ .

LENGTHSCALE $c = l$	0.05	0.1	0.3	0.9
$F_{\text{PriorVAE}}$	45.47	37.48	8.29	22.94
$F_{\text{PriorCVAE}}$	14.45	7.63	6.42	1.99

**MCMC Inference.** A ground truth curve was generated using the lengthscale  $l_{\text{true}} = 0.2$ . To generate observed data, we selected four locations and added a random amount of noise at each of the locations, distributed as  $s \sim \mathcal{N}^+(0.1)$ . We fit three models to this data using the NUTS sampler using three different priors:  $f_{\text{GP}}$ ,  $f_{\text{PriorVAE}}$  and  $f_{\text{PriorCVAE}}$ . Figure 6 presents the results of inference by overlaying the means and BCIs of the three models. All the estimated means are close to each other, but the BCIs of the PriorCVAE are much closer to the GP BCIs than the BCIs from PriorVAE. Most importantly, PriorCVAE’s BCIs have the same shape as the BCIs produced by the GP and the gap can be adjusted for at the inference stage by introducing slightly more liberal priors for amplitude. The BCIs of PriorVAE are narrower and have a different characteristic shape. For instance, in the interval from  $x = 0.7$  to  $x = 0.8$ , i.e. between the two rightmost data points, the amount of uncertainty does not increase in the areas away from the observed data - a behaviour expected from a GP. All three models were run using 5000 warm-up steps, 50000 post warm-up iterations<sup>2</sup> and 3 chains. Evaluation of run times, number of effective steps and number of effective steps per second are presented in Table 2. The number of effective steps of PriorCVAE per second is 10K times higher than the one of the original GP model, while the lengthscale parameter can also be recovered. Figure 7 presents posterior estimates of the lengthscale parameter produced by PriorCVAE and GP models and they are in good agreement. Using the same implementation software Numpyro (Phan et al., 2019; Bingham et al., 2019) as for the above models, we performed inference using popular approximation techniques - Laplace approximation and automatic differentiation variational inference (ADVI) (Kucukelbir et al., 2017). Results presented in Figure 8 show that ADVI failed at estimating both the mean and the lengthscale; Laplace

<sup>2</sup>PriorVAE and PriorCVAE models require much fewer iterations for convergence. These high values are required for the GP model to converge and, hence, have been set equal for all three models.

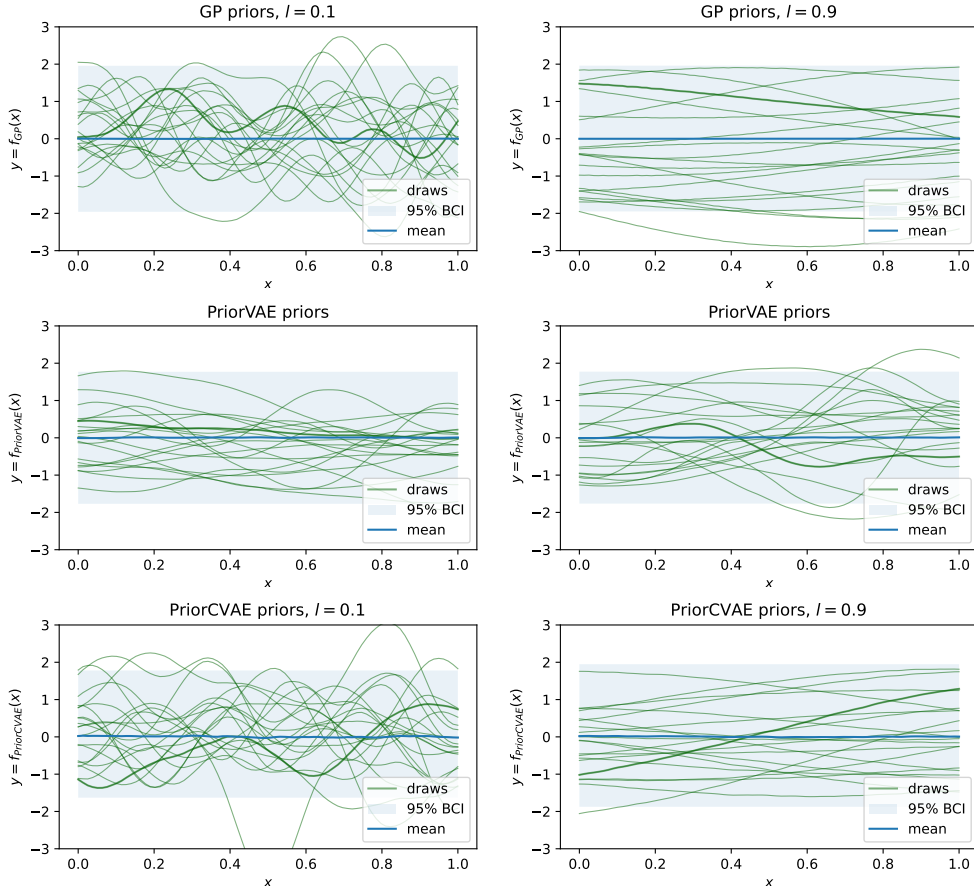


Figure 4: Visual diagnostics of the priors learned by PriorCVAE with continuous condition  $c = l$ , demonstrated for a short lengthscale  $l = 0.1$  (left) and a long lengthscale  $l = 0.9$  (right). Top row: original GP priors; middle row: VAE priors; bottom row: CVAE priors.

Table 2: Comparison of PriorVAE, PriorCVAE and GP inference results: number of effective steps, elapsed time, and number of effective steps per second. Neff per second for PriorCVAE is 10K times higher than the one of the GP.

MODEL	NEFF	ELAPSED TIME, S	NEFF/S
PRIORVAE	31115	8	3889
PRIORCVAE	34725	17	<b>2043</b>
GP	1496	7150	<b>0.2</b>

approximation is able to estimate the mean well, but produced no characterisation of uncertainty, as well as only a point estimate for the lengthscale<sup>3</sup>.

<sup>3</sup>Uncertainty estimation results produced by Laplace approximation differ depending on the hardware: on Google Colab, the uncertainty is present, but the BCI intervals have no variation in width depending on the distance from observed point; on a laptop, no uncertainty is produced at all.

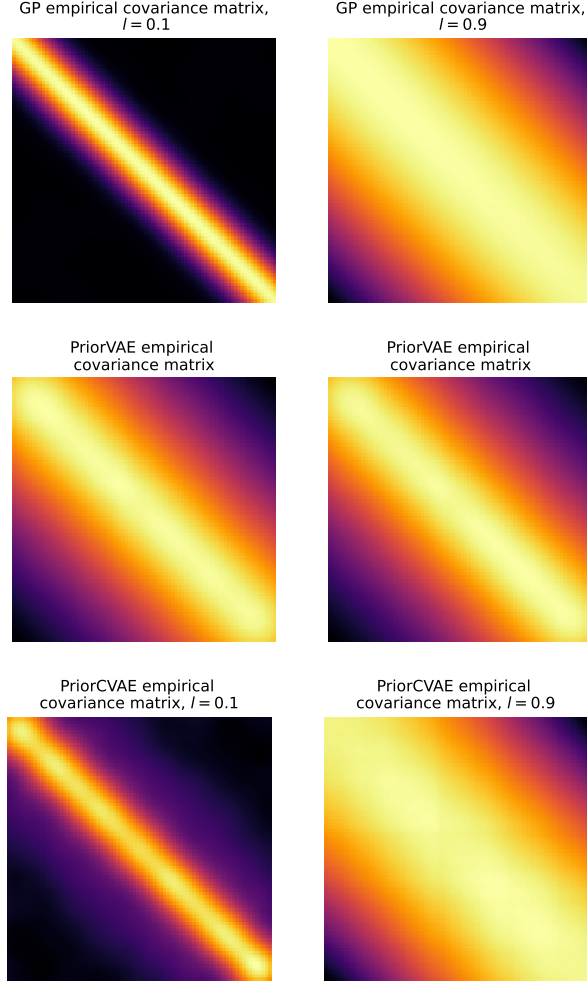


Figure 5: Empirical covariance matrices of the original  $f_{\text{GP}}$  priors (top), PriorVAE priors  $f_{\text{PriorVAE}}$  (middle) and PriorCVAE priors  $f_{\text{PriorCVAE}}$  (bottom). GP and PriorCVAE priors are conditioned on the short lengthscale  $l = 0.1$  (left) and the long lengthscale  $l = 0.9$  (right).

### 4.3 Encoding non-stationary kernels

In this section we will show for the first time that prior-encoding VAEs are also able to learn non-stationary GPs. Consider a kernel which is a product of linear and RBF kernels:

$$\begin{aligned}
 k_{\text{lin}}(s_i, s_j) &= (s_i - c_{\text{lin}})(s_j - c_{\text{lin}}), \\
 k_{\text{rbf}}(s_i, s_j) &= \exp\left(-\frac{\|s_i - s_j\|^2}{l^2}\right), \\
 k(s_i, s_j) &= k_{\text{lin}}(s_i, s_j)k_{\text{rbf}}(s_i, s_j) \\
 &= (s_i - c_{\text{lin}})(s_j - c_{\text{lin}}) \exp\left(-\frac{\|s_i - s_j\|^2}{l^2}\right).
 \end{aligned}$$

We keep the value of parameter  $c_{\text{lin}} = 0.4$  fixed and, as before, aim to encode the lengthscale as the condition. This time, the model generating data uses a narrower prior:  $l \sim \mathcal{U}(0.01, 0.4)$ , instead of  $l \sim \mathcal{U}(0.01, 0.99)$ , in order to test extrapolation abilities of PriorCVAE. Visual assessment of the quality of the learned priors is presented in Figure 9, which corresponds to two lengthscales contained in the  $(0.01, 0.4)$  interval: 0.2 (a

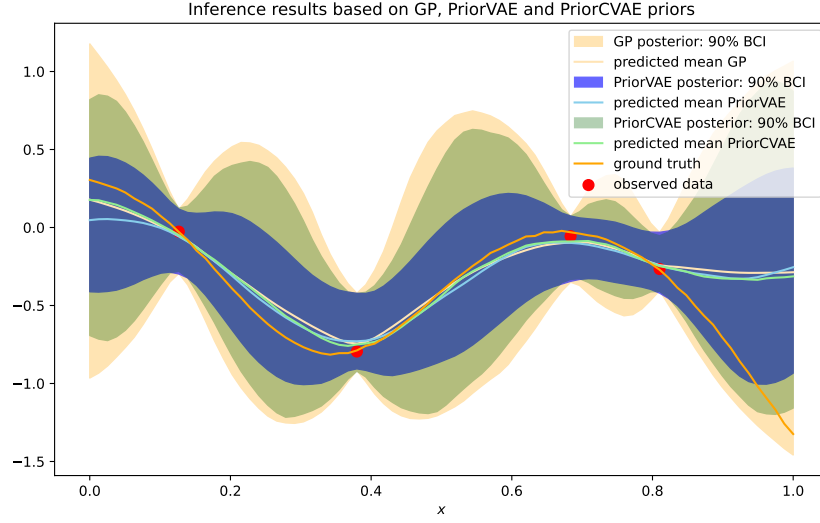


Figure 6: Comparing inference results produced by GP, PriorVAE and PriorCVAE models. Estimated means of all models agree well; 90% BCIs of PriorCVAE are closer to those of the GP than PriorVAE.

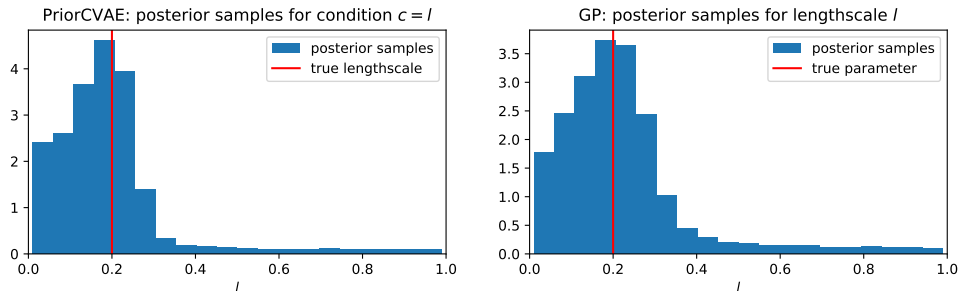


Figure 7: Posterior samples of the lengthscale obtained from the model with GP prior (left) and PriorCVAE prior (right).

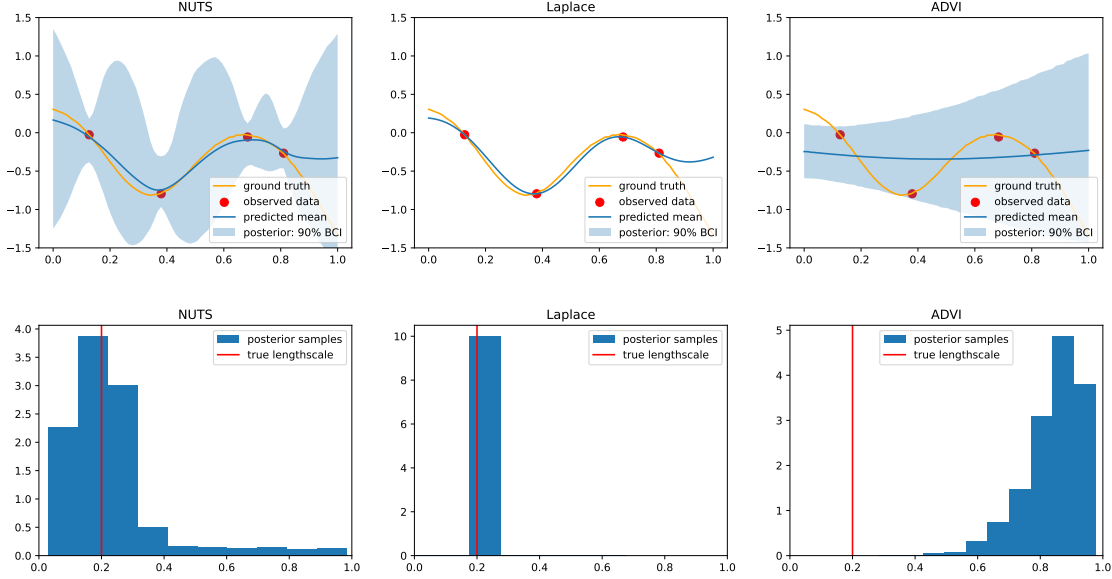


Figure 8: Comparing NUTS, Laplace and ADVI inference results on a one-dimensional Gaussian Process. Top: inferred mean and 90% BCI, bottom: inferred lengthscale.

typical value) and 0.05 (a value close to the border of the interval). The corresponding empirical covariance matrices are shown in Figure 14.

**Neural network training details.** CVAE architecture is identical to the two experimentst above. The neural network was trained for  $n_{\text{epochs}} = 1000$  epochs, with  $n_{\text{batch}} = 1000$  batch size, and  $1e^{-3}$  learning rate. Value of the  $\sigma_{\text{vae}}^2$  hyperparameter was set to 0.1. Training of the neural network took 16 minutes.

**Extrapolation of hyperparameters.** Even though we only trained the decoder with lengthscales drawn from  $(0.01, 0.4)$  interval, it is possible to condition PriorCVAE draws on lengthscales  $\tilde{l}$  which lie outside of this interval. Figure 10 compares the quality of extrapolation for  $\tilde{l} = 0.5$  and  $\tilde{l} = 0.9$ , showing that the prior quality is high close to the interval, and deteriorates for  $\tilde{l}$  further away.

#### 4.4 Encoding integral of the intensity function of the log-Gaussian Cox process $\int_D \exp(f(s))ds$

Similarly to other prior-encoding VAEs, PriorCVAE is able to encode function properties alongside function realisations. The integral

$$\mathcal{I} = \int_D \exp(f(s))ds, s \in D$$

is a crucial quantity required to evaluate log-Gaussian Cox process (LGCP) likelihood (Møller et al., 1998). LGCP is defined by an intensity function

$$\lambda(s) = \exp(f(s)), \quad f(s) \sim \mathcal{GP}(\cdot, \cdot)$$

which is Gaussian on the log-scale. The log-likelihood of an observed point pattern  $S$ , i.e. a collection of observed event locations  $S = \{s_1, s_2, \dots, s_N\}, s_j \in D$ , can then be written as  $L(\lambda|s_1, s_2, \dots, s_N) = \exp(-\int_D \lambda(s)ds) \prod_{j=1}^N \lambda(s_j)$ . Therefore, the log-likelihood involves the integral of the intensity function over the whole observation domain  $\mathcal{I} := \int_D \lambda(s)ds = \int_D \exp(f(s))ds$ . The presence of this term makes LGCP inference challenging. Here we demonstrate in one-dimensional case  $D = (0, 1)$  that the integral  $\mathcal{I}$  can be encoded jointly with the GP realisations and recovered at inference. Implementation details are

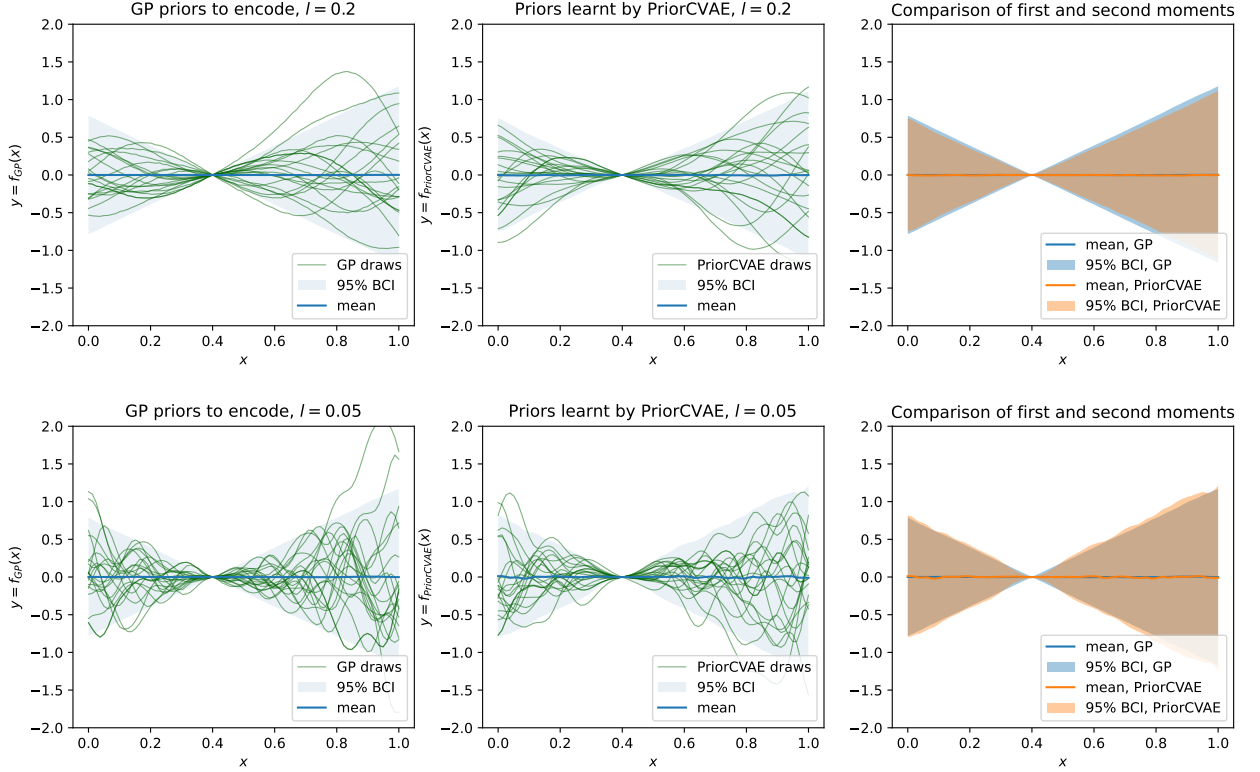


Figure 9: Priors drawn from a GP with a non-stationary kernel (left column) and priors learned by PriorCVAE (middle column). At training, lengthscales are drawn from the interval  $\mathcal{U}(0.01, 0.4)$ . Top row:  $l = 0.2$  (a typical value), bottom row:  $l = 0.05$  (a value close to the border of the interval). The rightmost column overlays the first and second moments of the GP and PriorCVAE priors, and they are in excellent agreement.

provided in A.2. The objective now includes an additional term - reconstruction loss of the integral value:

$$\begin{aligned} \mathcal{L}_{\text{PriorCVAE}} = & \frac{1}{2\sigma_{f,\text{VAE}}^2} \text{MSE}(f_{\text{GP}}, f_{\text{PriorCVAE}}) \\ & + \frac{1}{2\sigma_{\mathcal{I},\text{VAE}}^2} \text{MSE}(\mathcal{I}_{\text{GP}}, \mathcal{I}_{\text{PriorCVAE}}) \\ & - KL[\mathcal{N}(\mu_z, \sigma_z^2 I_d) || \mathcal{N}(0, I_d)], \end{aligned}$$

where

$$\begin{aligned} \mathcal{I}_{\text{GP}} & \approx \frac{1}{n} \sum_{i=1}^n f_{\text{GP}}^i, \quad f_{\text{GP}}^i = f(g_i), \quad \{g_i\}_{i=1}^n - \text{computational grid}, \\ \mathcal{I}_{\text{PriorCVAE}} & \approx \frac{1}{n} \sum_{i=1}^n f_{\text{PriorCVAE}}^i, \end{aligned}$$

and  $\sigma_{f,\text{VAE}}$  and  $\sigma_{\mathcal{I},\text{VAE}}$  are two different tuning parameters. In this experiment we have focused on GP samples with RBF kernel and  $l = 0.2$ . To assess the quality of the integral estimation by the decoder, we compare  $\mathcal{I}_{\text{PriorCVAE}}$  with the value of the integral computed from the recovered  $f_{\text{PriorCVAE}}$  samples. The benefit of such encoding is that if a more complex quadrature is required, it would be performed prior to inference and not during it, even if the evaluations  $f_{\text{GP}}$  are no longer costly. We fix one curve for which we know the true value of the integral computed via the same quadrature rule. Then we iterate through the number of observed points from 5 to 70 in increments of 5 points, and fit the PriorCVAE model to the data five times. Results are presented on Figure 15. For any assessed number of observed points, the mean

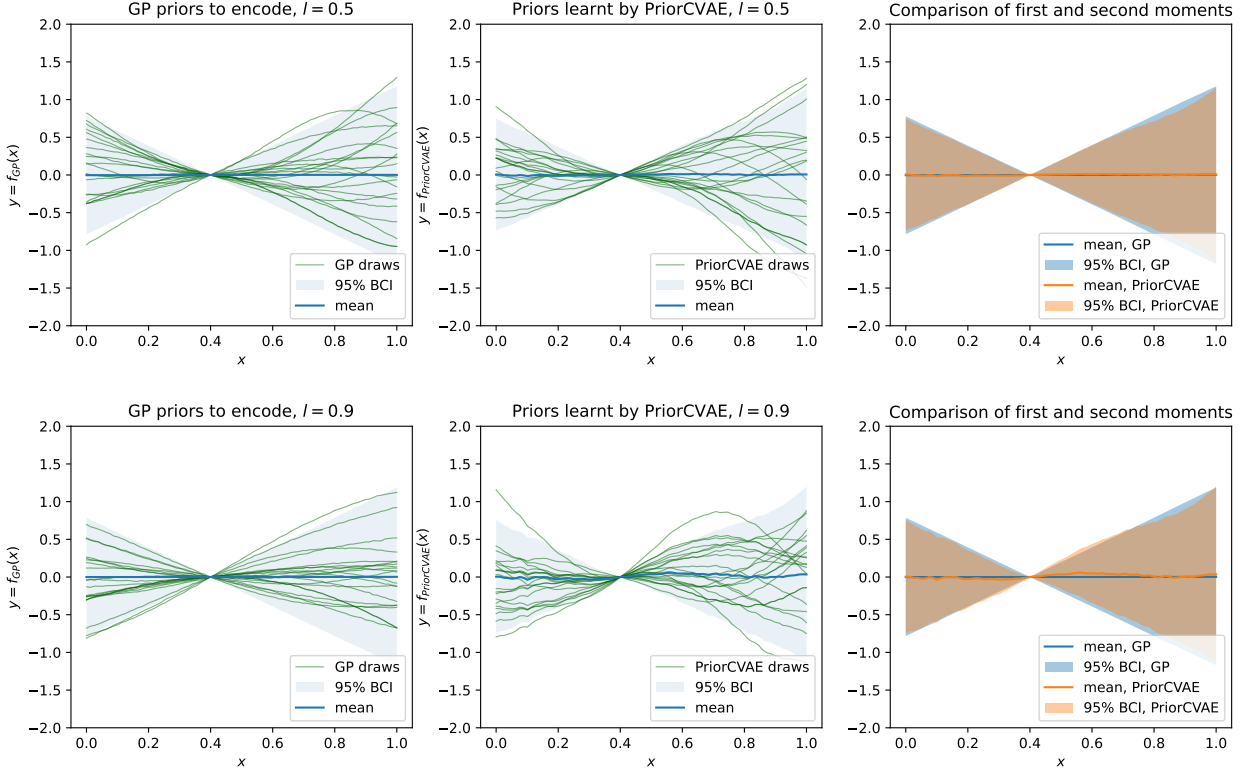


Figure 10: PriorCVAE is able to extrapolate with respect to hyperparameters and draw priors corresponding to unseen lengthscales  $\tilde{l}$ . The closer  $\tilde{l}$  is to the range of the values seen by the decoder, the better the quality of priors ( $\tilde{l} = 0.5$  in the top row); while the quality deteriorates for  $\tilde{l}$  further from the interval ( $\tilde{l} = 0.9$  in the bottom row)

estimates produced by the two approaches differ by at most 0.1. The same statement holds for uncertainty intervals. Here we used the simplest quadrature scheme, however, other quadratures could be used, without adding extra computational cost to the inference step.

## 5 Discussion and future work

In this paper we introduced PriorCVAE, a method based on deep generative modelling that enables explicit parameter estimation while performing fast and efficient MCMC inference. It covers the gap in the literature on encoding stochastic processes and their finite evaluations, where information about underlying parameters is completely lost. We solved the problem by conditioning the generative process on the parameters of interest and demonstrated that the conditioning can be performed both by categorical and continuous parameters. PriorCVAE retains the advantages of PriorVAE at the inference stage, i.e. shorter computation times and higher effective samples size than an equivalent model fully inferred with MCMC, while, at the same time, allows explicit inference of hyperparameters.

Therefore, the new method bridges the gap between performance at inference and interpretability. Side-by-side comparison of the GP, PriorVAE and PriorCVAE models has shown that although PriorCVAE is less efficient than PriorVAE, it is inferring an additional parameter and, hence, can better reconstruct the underlying model; furthermore, the number of effective steps per seconds achieved by PriorCVAE is about 10K higher as compared to the GP. Using the non-stationary GP example, we demonstrated that it is possible to perform extrapolation with respect to hyperparameters; that the quality of reconstructed priors remains



---

high if the out-of-sample hyperparameter values are close to those in-sample and the quality of reconstruction deteriorates with distance.

We quantified the quality of the learnt PriorVAE and PriorCVAE priors by measuring distance of their empirical covariance matrices to the one of the original GP prior. Table 1 showed that this form of quantification agrees with the results obtained at inference, i.e. that PriorCVAE priors match GP priors better than PriorVAE. Future work includes extensions where Frobenius norm constitutes a part of the reconstruction loss to match second moments, or maximum mean discrepancy (Gretton et al., 2012) could be used to match higher moments by design.

All examples presented in the current paper extend the PriorVAE workflow to learn finite evaluations of stochastic processes. Future work includes adoption of this approach to  $\pi$ VAE in order to encode not just vectors, but stochastic processes while retaining the ability to infer parameters. The three key features of PriorCVAE - speed, efficiency and ability to estimate parameters within MCMC - make this method preferable to existing state of the art approximate techniques. Hence, we believe that PriorCVAE and its extensions have the potential to make a major impact in spatial statistics and related domains requiring inference over correlated structures. Immediate potential for applications includes encoding of time series data, as well as expanding the list of kernels that the method has been applied to.

## Acknowledgments

E.S. and S.F. acknowledge the EPSRC (EP/V002910/1). E.S. acknowledges supported in part by the AI2050 program at Schmidt Futures (Grant [G-22-64476]).

## References

- Seth D Axen, Alexandra Gessner, Christian Sommer, Nils Weitzel, and Álvaro Tejero-Cantero. Spatiotemporal modeling of european paleoclimate using doubly sparse gaussian processes. *arXiv preprint arXiv:2211.08160*, 2022.
- Santiago Belda, Luca Pipia, Eatidal Amin, Matías Salinero, Pablo Reyes, and Jochem Verrelst. Crop phenology retrieval through gaussian process regression. In *2021 IEEE International Geoscience and Remote Sensing Symposium IGARSS*, pp. 6256–6259. IEEE, 2021.
- Julian Besag. Spatial interaction and the statistical analysis of lattice systems. *Journal of the Royal Statistical Society: Series B (Methodological)*, 36(2):192–225, 1974.
- Julian Besag, Jeremy York, and Annie Mollié. Bayesian image restoration, with two applications in spatial statistics. *Annals of the institute of statistical mathematics*, 43(1):1–20, 1991.
- Eli Bingham, Jonathan P. Chen, Martin Jankowiak, Fritz Obermeyer, Neeraj Pradhan, Theofanis Karaletsos, Rohit Singh, Paul A. Szerlip, Paul Horsfall, and Noah D. Goodman. Pyro: Deep universal probabilistic programming. *J. Mach. Learn. Res.*, 20:28:1–28:6, 2019. URL <http://jmlr.org/papers/v20/18-403.html>.
- David M Blei, Alp Kucukelbir, and Jon D McAuliffe. Variational inference: A review for statisticians. *Journal of the American statistical Association*, 112(518):859–877, 2017.
- Sam Bond-Taylor, Adam Leach, Yang Long, and Chris G Willcocks. Deep generative modelling: A comparative review of vaes, gans, normalizing flows, energy-based and autoregressive models. *arXiv preprint arXiv:2103.04922*, 2021.
- James Bradbury, Roy Frostig, Peter Hawkins, Matthew James Johnson, Chris Leary, Dougal Maclaurin, George Necula, Adam Paszke, Jake VanderPlas, Skye Wanderman-Milne, and Qiao Zhang. JAX: composable transformations of Python+NumPy programs, 2018. URL <http://github.com/google/jax>.
- David S Broomhead and David Lowe. Radial basis functions, multi-variable functional interpolation and adaptive networks. Technical report, Royal Signals and Radar Establishment Malvern (United Kingdom), 1988.

- 
- Bob Carpenter, Andrew Gelman, Matthew D Hoffman, Daniel Lee, Ben Goodrich, Michael Betancourt, Marcus Brubaker, Jiqiang Guo, Peter Li, and Allen Riddell. Stan: A probabilistic programming language. *Journal of statistical software*, 76(1), 2017.
- Tao Dai, Sarah M Jordaan, and Aaron P Wemhoff. Gaussian process regression as a replicable, streamlined approach to inventory and uncertainty analysis in life cycle assessment. *Environmental Science & Technology*, 56(6):3821–3829, 2022.
- Marc Peter Deisenroth, Dieter Fox, and Carl Edward Rasmussen. Gaussian processes for data-efficient learning in robotics and control. *IEEE transactions on pattern analysis and machine intelligence*, 37(2):408–423, 2013.
- Vincent Dutordoir, Alan Saul, Zoubin Ghahramani, and Fergus Simpson. Neural diffusion processes. *arXiv preprint arXiv:2206.03992*, 2022.
- Hong Ge, Kai Xu, and Zoubin Ghahramani. Turing: a language for flexible probabilistic inference. In *International conference on artificial intelligence and statistics*, pp. 1682–1690. PMLR, 2018.
- Andrew Gelman, John B Carlin, Hal S Stern, and Donald B Rubin. *Bayesian data analysis*. Chapman and Hall/CRC, 1995.
- Arthur Gretton, Karsten M Borgwardt, Malte J Rasch, Bernhard Schölkopf, and Alexander Smola. A kernel two-sample test. *The Journal of Machine Learning Research*, 13(1):723–773, 2012.
- Irina Higgins, Loic Matthey, Arka Pal, Christopher Burgess, Xavier Glorot, Matthew Botvinick, Shakir Mohamed, and Alexander Lerchner. beta-VAE: Learning basic visual concepts with a constrained variational framework. In *International Conference on Learning Representations*, 2017. URL <https://openreview.net/forum?id=Sy2fzU9gl>.
- Matthew D. Hoffman and Andrew Gelman. The no-u-turn sampler: Adaptively setting path lengths in hamiltonian monte carlo. *Journal of Machine Learning Research*, 15(47):1593–1623, 2014. URL <http://jmlr.org/papers/v15/hoffman14a.html>.
- Noah Hollmann, Samuel Müller, Katharina Eggersperger, and Frank Hutter. TabPFN: A transformer that solves small tabular classification problems in a second. *arXiv preprint arXiv:2207.01848*, 2022.
- Gavin Kerrigan, Justin Ley, and Padhraic Smyth. Diffusion generative models in infinite dimensions. *arXiv preprint arXiv:2212.00886*, 2022.
- Diederik P Kingma and Jimmy Ba. Adam: A method for stochastic optimization. *arXiv preprint arXiv:1412.6980*, 2014.
- Diederik P Kingma and Max Welling. Auto-encoding variational bayes. *arXiv preprint arXiv:1312.6114*, 2013.
- Andreas Krause and Carlos Guestrin. Nonmyopic active learning of gaussian processes: an exploration-exploitation approach. In *Proceedings of the 24th international conference on Machine learning*, pp. 449–456, 2007.
- Alp Kucukelbir, Dustin Tran, Rajesh Ranganath, Andrew Gelman, and David M Blei. Automatic differentiation variational inference. *Journal of machine learning research*, 2017.
- Swapnil Mishra, Seth Flaxman, Tresnia Berah, Mikko Pakkanen, Harrison Zhu, and Samir Bhatt. *pi* vae: Encoding stochastic process priors with variational autoencoders. *Statistics & Computing*, 2022.
- Jesper Møller, Anne Randi Syversveen, and Rasmus Plenge Waagepetersen. Log gaussian cox processes. *Scandinavian journal of statistics*, 25(3):451–482, 1998.
- Olga Obrezanova, Gábor Csányi, Joelle MR Gola, and Matthew D Segall. Gaussian processes: a method for automatic qsar modeling of adme properties. *Journal of chemical information and modeling*, 47(5):1847–1857, 2007.

- 
- Adam Paszke, Sam Gross, Francisco Massa, Adam Lerer, James Bradbury, Gregory Chanan, Trevor Killeen, Zeming Lin, Natalia Gimelshein, Luca Antiga, et al. Pytorch: An imperative style, high-performance deep learning library. *Advances in neural information processing systems*, 32, 2019.
- Du Phan, Neeraj Pradhan, and Martin Jankowiak. Composable effects for flexible and accelerated probabilistic programming in numpyro. *arXiv preprint arXiv:1912.11554*, 2019.
- John NK Rao and Isabel Molina. *Small area estimation*. John Wiley & Sons, 2015.
- Danilo Jimenez Rezende, Shakir Mohamed, and Daan Wierstra. Stochastic backpropagation and approximate inference in deep generative models. In *International conference on machine learning*, pp. 1278–1286. PMLR, 2014.
- Andrea Riebler, Sigrunn H Sørbye, Daniel Simpson, and Håvard Rue. An intuitive bayesian spatial model for disease mapping that accounts for scaling. *Statistical methods in medical research*, 25(4):1145–1165, 2016.
- Christian P Robert, George Casella, and George Casella. *Monte Carlo statistical methods*, volume 2. Springer, 1999.
- Timon S Schroeter, Anton Schwaighofer, Sebastian Mika, Antonius Ter Laak, Detlev Suelzle, Ursula Ganzer, Nikolaus Heinrich, and Klaus-Robert Müller. Predicting lipophilicity of drug-discovery molecules using gaussian process models. *ChemMedChem: Chemistry Enabling Drug Discovery*, 2(9):1265–1267, 2007.
- Elizaveta Semenova, Maria Luisa Guerriero, Bairu Zhang, Andreas Hock, Philip Hopcroft, Ganesh Kadamur, Avid M Afzal, and Stanley E Lazic. Flexible fitting of protac concentration–response curves with change-point gaussian processes. *SLAS DISCOVERY: Advancing the Science of Drug Discovery*, 26(9):1212–1224, 2021.
- Elizaveta Semenova, Yidan Xu, Adam Howes, Theo Rashid, Samir Bhatt, Swapnil Mishra, and Seth Flaxman. Priorvae: encoding spatial priors with variational autoencoders for small-area estimation. *Journal of the Royal Society Interface*, 19(191):20220094, 2022.
- Yuliya Shapovalova, Tom Heskes, and Tjeerd Dijkstra. Non-parametric synergy modeling of chemical compounds with gaussian processes. *BMC bioinformatics*, 23:1–30, 2022.
- Kihyuk Sohn, Honglak Lee, and Xinchun Yan. Learning structured output representation using deep conditional generative models. *Advances in neural information processing systems*, 28, 2015.
- Jakub M Tomczak. Deep generative modeling for neural compression. In *Deep Generative Modeling*, pp. 173–188. Springer, 2022.
- Aki Vehtari, Andrew Gelman, Daniel Simpson, Bob Carpenter, and Paul-Christian Bürkner. Rank-normalization, folding, and localization: an improved r for assessing convergence of mcmc (with discussion). *Bayesian analysis*, 16(2):667–718, 2021.
- Martin J Wainwright and Michael I Jordan. Introduction to variational methods for graphical models. *Foundations and Trends in Machine Learning*, 1:1–103, 2008.
- Martin J Wainwright, Michael I Jordan, et al. Graphical models, exponential families, and variational inference. *Foundations and Trends® in Machine Learning*, 1(1–2):1–305, 2008.
- Christopher KI Williams and Carl Edward Rasmussen. *Gaussian processes for machine learning*, volume 2. MIT Press, Cambridge, MA, 2006.
- Abraham Noah Wu and Filip Biljecki. Instantcity: Synthesising morphologically accurate geospatial data for urban form analysis, transfer, and quality control. *ISPRS Journal of Photogrammetry and Remote Sensing*, 195:90–104, 2023.

Jiaxuan You, Xiaocheng Li, Melvin Low, David Lobell, and Stefano Ermon. Deep gaussian process for crop yield prediction based on remote sensing data. In *Thirty-First AAAI conference on artificial intelligence*, 2017.

Guangyao Zhou. Mixed hamiltonian monte carlo for mixed discrete and continuous variables. *Advances in Neural Information Processing Systems*, 33:17094–17104, 2020.

## A Appendix

### A.1 Software

A GitHub repository with a Python environment and code to reproduce the experiments is ready to be shared. The neural network models were implemented with PyTorch Paszke et al. (2019) in Python. Bayesian inference, including NUTS, Laplace approximation and ADVI, were implemented in Numpyro Phan et al. (2019); Bingham et al. (2019) using JAX Bradbury et al. (2018) as the backend.

### A.2 Encoding $\int \exp(f(x))dx$ : implementation details

Here  $\log\text{-sum-exp}(v) = \log(\sum_{i=1}^n \exp(v_i)) = \max(v) + \log[\sum_{i=1}^n \exp(v_i - \max(v))]$ .

### A.3 Supplementary figures.

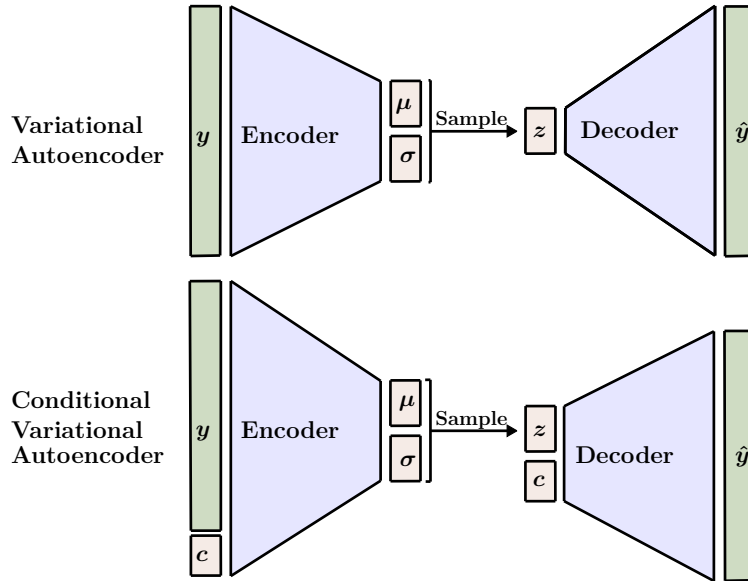


Figure 11: VAE versus CVAE architectures. Both encoder and decoder get the label  $c$  as input. Traditionally,  $c$  is an observed class label. Here we interpret  $c$  as a hyperparameter of the prior.

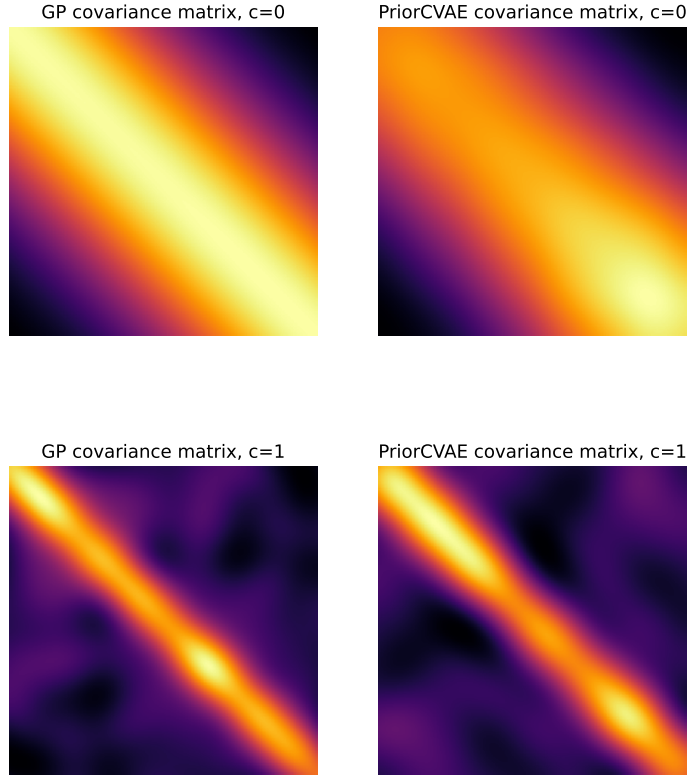


Figure 12: Visual diagnostics of the priors learned by PriorCVAE and the original GP priors corresponding to the standardised RBF kernel: empirical covariance matrices. Left column: covariance matrices computed using samples from the original Gaussian process evaluations  $f_{\text{GP}}$ , right column: covariance matrices computed using the samples drawn from  $f_{\text{CVAE}}$  trained on  $f_{\text{GP}}$  draws. Top row: samples corresponding to the condition  $c = 0$ , bottom row: samples corresponding to the condition  $c = 1$ .

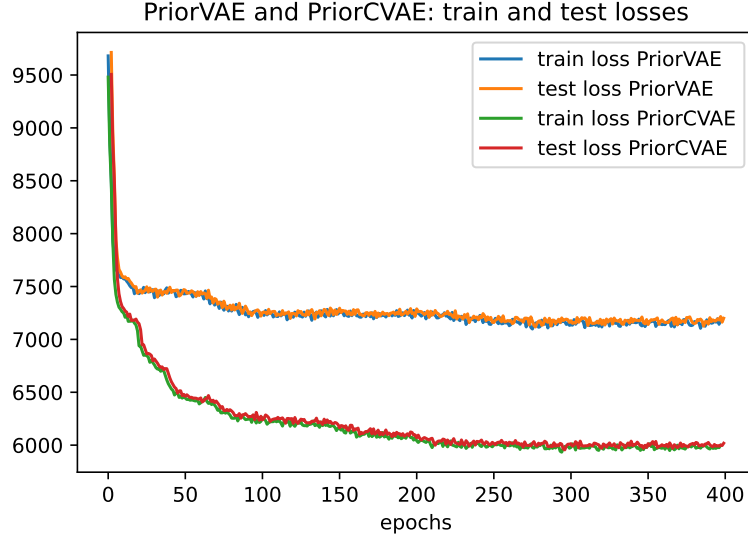


Figure 13: Training and test losses of PriorVAE and PriorCVAE models.

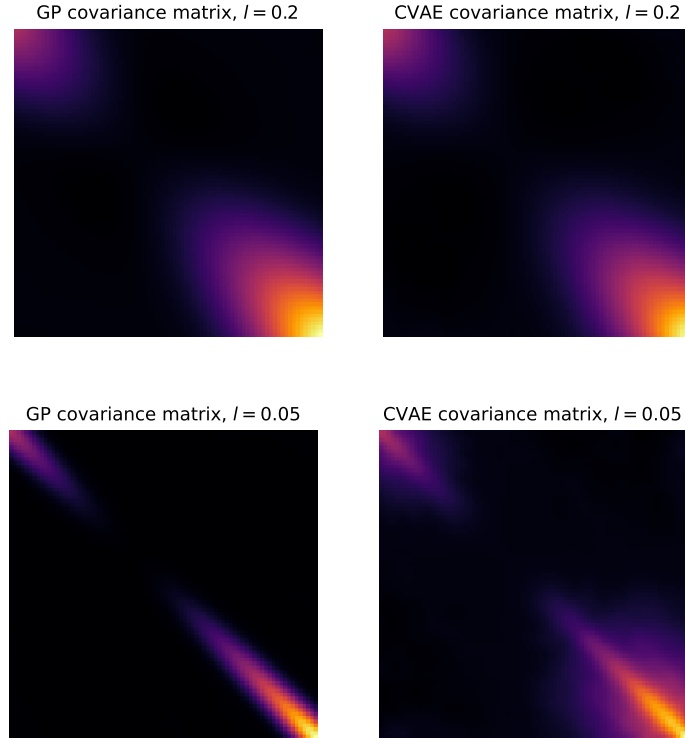


Figure 14: Empirical covariance matrices of the non-stationary  $f_{\text{GP}}$  and PriorCVAE priors trained using values  $l \sim U(0.01, 0.4)$ . Top row corresponds to  $l = 0.2$  (a typical value), bottom row corresponds to 0.05 (a value close to the border of the interval).

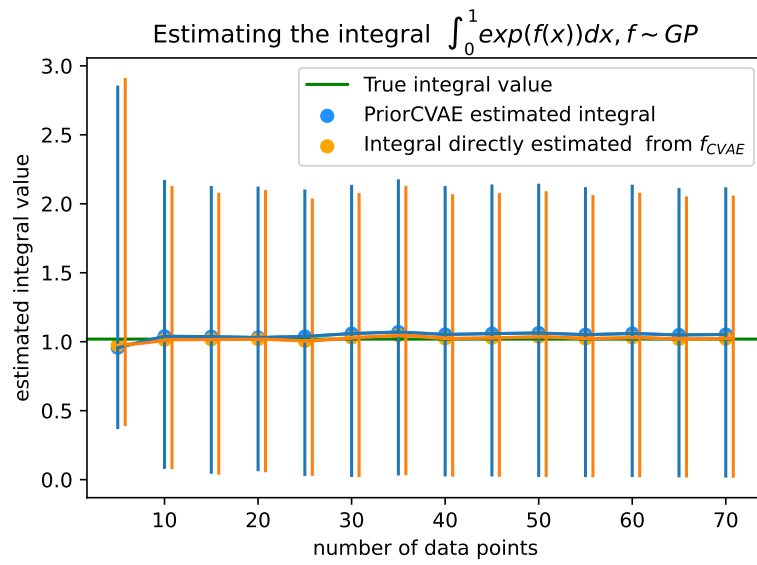


Figure 15: Encoding  $\int_0^1 \exp(f(x)) dx$